iScience

CellPress
OPEN ACCESS

Article

Mosaic ablation of pancreatic β cells induces de-differentiation and repetitive proliferation of residual β cells in adult mice

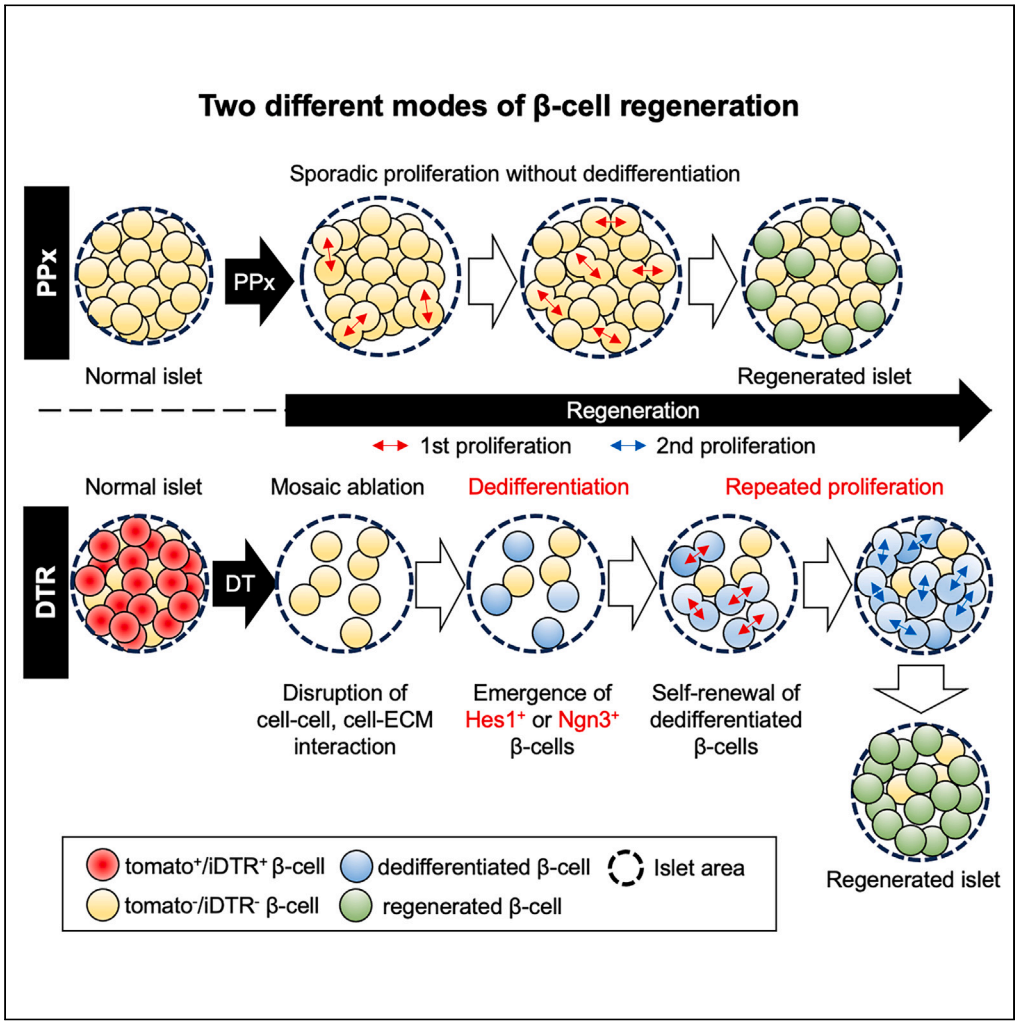

Ryo Hatano, Xilin Zhang, Eunyoung Lee, Atsushi Kaneda, Tomoaki Tanaka, Takashi Miki

tmiki@faculty.chiba-u.jp (T.M.)
hatanori@chiba-u.jp (R.H.)

Highlights

Dedifferentiated residual β cells proliferate repeatedly after mosaic β cell ablation

Partial pancreatectomy triggers sporadic β cell proliferation without dedifferentiation

The mode of β cell regeneration is affected by the islet microenvironment

Hatano et al., iScience 27, 110656
September 20, 2024
https://doi.org/10.1016/j.isci.2024.110656

iScience

CellPress
OPEN ACCESS

Article

Mosaic ablation of pancreatic β cells induces de-differentiation and repetitive proliferation of residual β cells in adult mice

Ryo Hatano,[1,5,*] Xilin Zhang,[1] Eunyoung Lee,[1,2] Atsushi Kaneda,[3] Tomoaki Tanaka,[2,4] and Takashi Miki[1,2,*]

SUMMARY

Diabetes mellitus is induced by quantitative and qualitative decline in pancreatic β cells. Although its radical therapy has not yet been established, β cell regeneration is a promising option. We investigate here two mouse models of β cell regeneration induced after ~80% reduction in β cell number: Cre/loxP-mediated β cell ablation and partial pancreatectomy. Cre/loxP-mediated, mosaic-pattern of β cell ablation by diphtheria toxin (DT) prompted rapid β cell replenishment through repeated proliferation of rare, highly proliferative DT receptor-negative β cells along with increase in *Hes1*, *Neurog3*, *Ascl1*, and *Aldh1a3* (immature/dedifferentiated β cell markers) and decrease in *Mafa* (a mature β cell marker) in the islets. In contrast, pancreatectomy also prompted active proliferation, but with no change in these immature/dedifferentiated or mature β cell markers. Our findings demonstrate that the mode of β cell regeneration differs between Cre/loxP-mediated β cell ablation and surgical β cell reduction, and the former involves β cell dedifferentiation followed by active repetitive cell proliferation of a small population of β cells.

INTRODUCTION

Pancreatic β cells play the central role in maintaining blood glucose homeostasis through timely insulin synthesis and secretion. Dysfunction and/or loss of β cells results in dysregulation of blood glucose and can trigger onset of diabetes mellitus (DM). Type 2 DM (T2DM) is a worldwide common metabolic disorder attributing to defective insulin secretion and/or insulin resistance. Decreased peripheral glucose uptake and augmented endogenous glucose production are hallmarks of insulin insufficiency. In addition, increased lipolysis in adipose tissue is linked to an increase in hepatic gluconeogenesis from glycerol.[1] Accordingly, numerous distinct factors are involved in the pathogenesis of T2DM. On the other hand, Butler et al. reported that increased apoptosis contributes to β cell loss which has already begun at early onset of T2DM patients.[2] Progressive reduction in β cell mass leads to further exacerbation of T2DM. While various categories of drugs have been developed to manage T2DM[3] and their purpose is to alleviate hyperglycemia, none of them addresses dysfunction or loss of β cells. A method of restoring functional β cells has long been desired to treat T2DM.

Numerous studies have been conducted to better understand β cell regeneration in conditions of reduced β cell mass. While proliferation of β cells occurs naturally in individuals during the fetal and neonatal period, it declines rapidly soon after birth.[4] In addition, proliferation of β cells occurs naturally in pregnancy, obesity, and insulin-resistant conditions.[5–7] In animal models, β cell regeneration has been found to occur after β cell-reduction procedures such as partial pancreatectomy (PPx), pancreatic duct ligation (PDL), and chemical ablation of β cells.[8–14] β cell number can be increased by replication of mature β cells, *trans*-differentiation of non-β cells to β cells, and proliferation of pre-existing stem/progenitor cells.[15] The mode by which β cell mass is replenished is influenced by the degree of decline: replication in conditions with little or mild β cell reduction and neogenesis after near-total ablation. In addition, extreme depletion of β cells has been reported to elicit β cell regeneration through *trans*-differentiation from α and δ cells.[16,17]

We previously generated β cell-specific DTR mice using rat insulin promotor (RIP) (rat *Ins2* promoter)-Cre mice (RIP-Cre: Rosa26 $^{iDTR/iDTR,\ tdtomato/+}$), in which we can induce mosaic-manner β cell deletion (Cre-mosaicism) upon DT administration.[18,19] In DTR mice, which express the diphtheria toxin receptor (DTR) specifically in 70~80% of the β cells,[19] DT administration results in robust proliferation of the DTR-negative β cells in mitigation of the loss, indicating both the necessity and sufficiency of a small number of intact, residual β cells for islet regeneration. However, the mode of proliferation and the cellular characteristics of the remaining β cells in DT-administered DTR mice during regeneration remain obscure. Cell-to-cell contact and other forms of local communication in a niche environment

[1]Department of Medical Physiology, Chiba University, Graduate School of Medicine, Chiba 260-8670, Japan
[2]Research Institute of Disaster Medicine (RIDM), Chiba University, Graduate School of Medicine, Chiba 260-8670, Japan
[3]Department of Molecular Oncology, Chiba University, Graduate School of Medicine, Chiba 260-8670, Japan
[4]Department of Molecular Diagnosis, Chiba University, Graduate School of Medicine, Chiba 260-8670, Japan
[5]Lead contact
*Correspondence: tmiki@faculty.chiba-u.jp (T.M.), hatanori@chiba-u.jp (R.H.)
https://doi.org/10.1016/j.isci.2024.110656

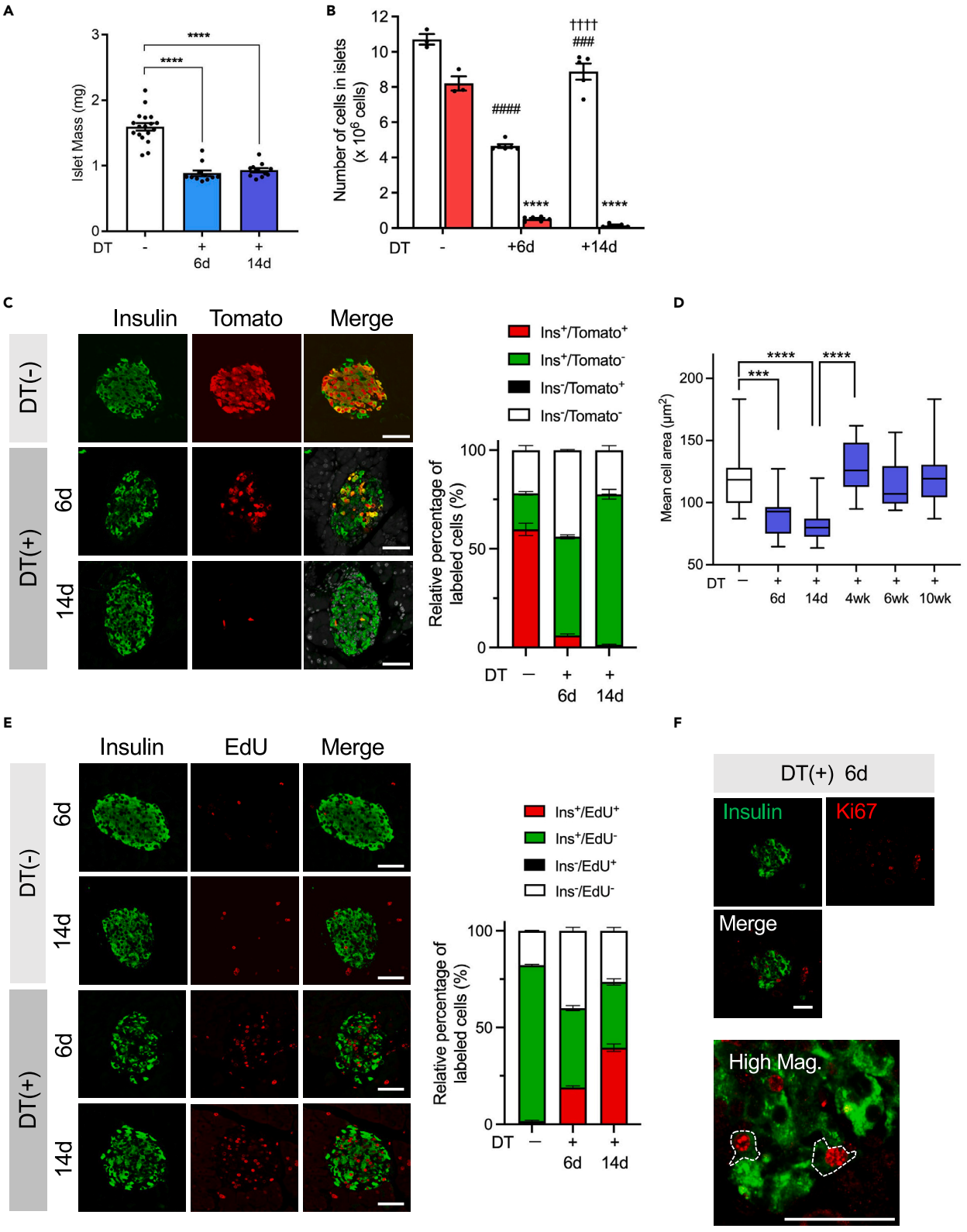
A
Islet Mass (mg)
****
****
DT
-
+ 6d
+ 14d
B
Number of cells in islets (x 10^6 cells)
####
****
††††
###
****
DT
-
+6d
+14d
C
Insulin
Tomato
Merge
DT(-)
DT(+)
6d
14d
Ins+/Tomato+
Ins+/Tomato-
Ins-/Tomato+
Ins-/Tomato-
Relative percentage of labeled cells (%)
DT
6d
14d
D
Mean cell area (μm2)
***
****
****
DT
6d
14d
4wk
6wk
10wk
E
Insulin
EdU
Merge
DT(-)
DT(+)
6d
14d
Ins+/EdU+
Ins+/EdU-
Ins-/EdU+
Ins-/EdU-
Relative percentage of labeled cells (%)
DT
6d
14d
F
DT(+) 6d
Insulin
Ki67
Merge
High Mag.

Figure 1. Histological changes in islets of DTR mice after β cell ablation by DT

(A) Quantification of islet mass (PBS-treated [DT−], on day 14, $n = 18$, in DT-treated [DT(+)] DTR mice [on day 6 (6 days): $n = 11$, on day 14 (14 days): $n = 11$]). ****$p < 0.0001$.

(B) Calculated total cell number in islets per pancreas of DTR mice. Insulin-positive (Ins^{+ve}) islet cell number (white bar), and Tomato-positive (Tom^{+ve})/Ins^{+ve} islet cell number (red bar) are shown. Data are expressed as mean ± SEM. ###$p < 0.001$, ####$p < 0.0001$: vs. Ins^{+ve} cell number in DT (−), ****$p < 0.0001$: vs. Tom^{+ve}/Ins^{+ve} cell number in DT (−), ††††$p < 0.0001$: vs. Ins^{+ve} cell number in DT(+) on day 6. DT(−): $n = 3$, DT+6 days: $n = 6$, DT+14 days: $n = 5$, respectively.

(C) Co-immunostaining of islets with tomato (Red) and insulin (green). DT(−):14 days after PBS injection; DT-treated DTR mice (6 or 14 days after DT injection). The percentages of labeled cells are displayed by bar plot. Data are expressed as mean ± SEM.

(D) Mean cell size in islets was calculated by dividing islet area by the number of Hoechst-positive nuclei. Data are expressed as mean ± SEM.

(E) Labeling of proliferated β cells by EdU. Six and 14 days after injection of PBS [DT(−)] or DT [DT(+)] in DTR mice (6 and 14 days after DT injection). The percentages of labeled cells are displayed by bar plot. Data are expressed as mean ± SEM.

(F) Co-immunostaining (Ki67 and insulin) of DTR mouse islet (6 days after DT injection). In a magnified image, Ki67-positive cells are surrounded by a dotted line within which weaker expression of insulin is observed. Scale bars: 50 μm.

has been reported to be critical in maintaining the state of stem/progenitor cells and induce their differentiation in various cell types,[20,21] suggesting that active β cell regeneration in DT-administered DTR mice may depend in part on the microenvironments induced by the mosaic-manner cell ablation as well as a degree of β cell number reduction. In this study, we compare β cell regeneration modes in our mosaic depletion model with those in a surgical resection model having a similar degree of β cell loss. While both models exhibit similar proliferative potential, they employ distinctly different modes of regeneration; repetitive proliferation of a small subset of the residual β cells together with increases in the premature β cell marker Ngn3 and the Notch-signal effector Hes1 in the DT-administered DTR mice but not in the PPx mice. These data indicate that differences in the microenvironments of the remaining β cells can induce distinct modes of repetitive proliferation of β cell progenitors to replenish β cell mass.

RESULTS

Pancreatic β cell ablation by DT induces proliferation of the unaffected β cells in DTR mice

We first measured islet mass (Figure 1A) and intra-islet cell number after β cell ablation in DT-administered DTR mice (Figure 1B). Islet mass (measurement of islet area) was reduced significantly 6 days after DT administration and remained low on day 14 (Figure 1A). In contrast, the number of insulin-positive (Ins^{+ve}) cells was decreased to 43 ± 1% of the DT-untreated (DT[−]) control on day 6 but recovered to 83 ± 3% on day 14 (Figure 1B, white columns). The number of Tomato-positive (Tom^{+ve}) cells (~70% of β cells in DT[−] control [Figure 1C]) was decreased markedly on day 6 with further decline on day 14 (Figure 1B, red columns), as shown on immunostaining images (Figure 1C). Thus, most of the DTR-positive (DTR^{+ve}) β cells were ablated by the single DT administration and β cell number recovered 2 weeks after the procedure. Although the number of Ins^{+ve} cells recovered to 80% by day 14, the islet mass remained low, suggesting that the size of the islet cells was less in these mice during this period. While the average cell size was found to be decreased significantly on day 6 and 14, it was normal at 4 weeks after DT administration (Figure 1D), coincident with the recovery in islet mass (Figure S1).

Visualization of the proliferated cells using the synthetic nucleoside analog EdU revealed an increase in EdU-positive (EdU^{+ve}) cells within the islets after DT administration to DTR mice (Figure 1E). In addition, most EdU^{+ve} cells were co-stained only weakly with insulin, suggesting that ablation had triggered cell division and that the proliferating β cells had become immature. Identification of proliferating cells by Ki67 immunostaining revealed that the Ki67-positive ($Ki67^{+ve}$) β cells were stained only weakly with insulin (Figure 1F). $Ki67^{+ve}$ cells were only sparsely observed until day 6 (Figure S2). Considering these findings together, the residual β cells may well begin proliferating soon after the procedure but lose maturity once the regeneration process is underway.

Recovery of β cell number after DT administration in DTR mice was mediated by the high capacity for proliferation of a small subset of the remaining β cells

Co-labeling with EdU plus Tomato in the islets of the DTR mice on day 6 and 14 after DT treatment revealed sustained proliferation of DTR-negative (DTR^{-ve}) β cells for up to 14 days (Figures 2A and 2B). Measurement of the EdU^{+ve} β cell number revealed that the number of proliferated β cells in 14 days had tripled, while that of non-proliferated β cells did not decrease (Figure 2C). If β cell division occurs randomly among the population of mature β cells, as was reported of β cell replication under unstimulated condition,[9] the relative number of non-proliferated β cells would be expected to decline as regeneration continues, as illustrated in Figure 2D (left). Our negative finding in this case indicates that a relatively small subset of cells contributed to the restoration of β cell mass in these mice (Figure 2D, right). In addition, the proportion of EdU^{+ve} cells peaked at 2 weeks after DT treatment and subsequently decreased (Figure S3). At 4 and 6 weeks, the incorporation rate of EdU or BrdU returned to basal levels, suggesting subsiding active β cell proliferation (Figure S4).

Remaining β cells in DT-administered DTR mice were immature, showing decreased MafA and increased markers of immaturity

Considering that $Ki67^{+ve}$ β cells in DT-treated DTR mice on day 6 were co-immunostained only weakly with insulin, these newly generated β cells are likely to be immature. Consistent with the current concept, MafA, a marker of mature β cells, was found to be expressed in many of the β cells in DT-untreated DTR mice (Figure 3A). However, the immunoreactivity of MafA was found to be markedly attenuated after DT administration on both day 6 and 14 in most of the cells within the islets, suggesting that DTR^{-ve} β cells had lost their maturity. In addition, the number

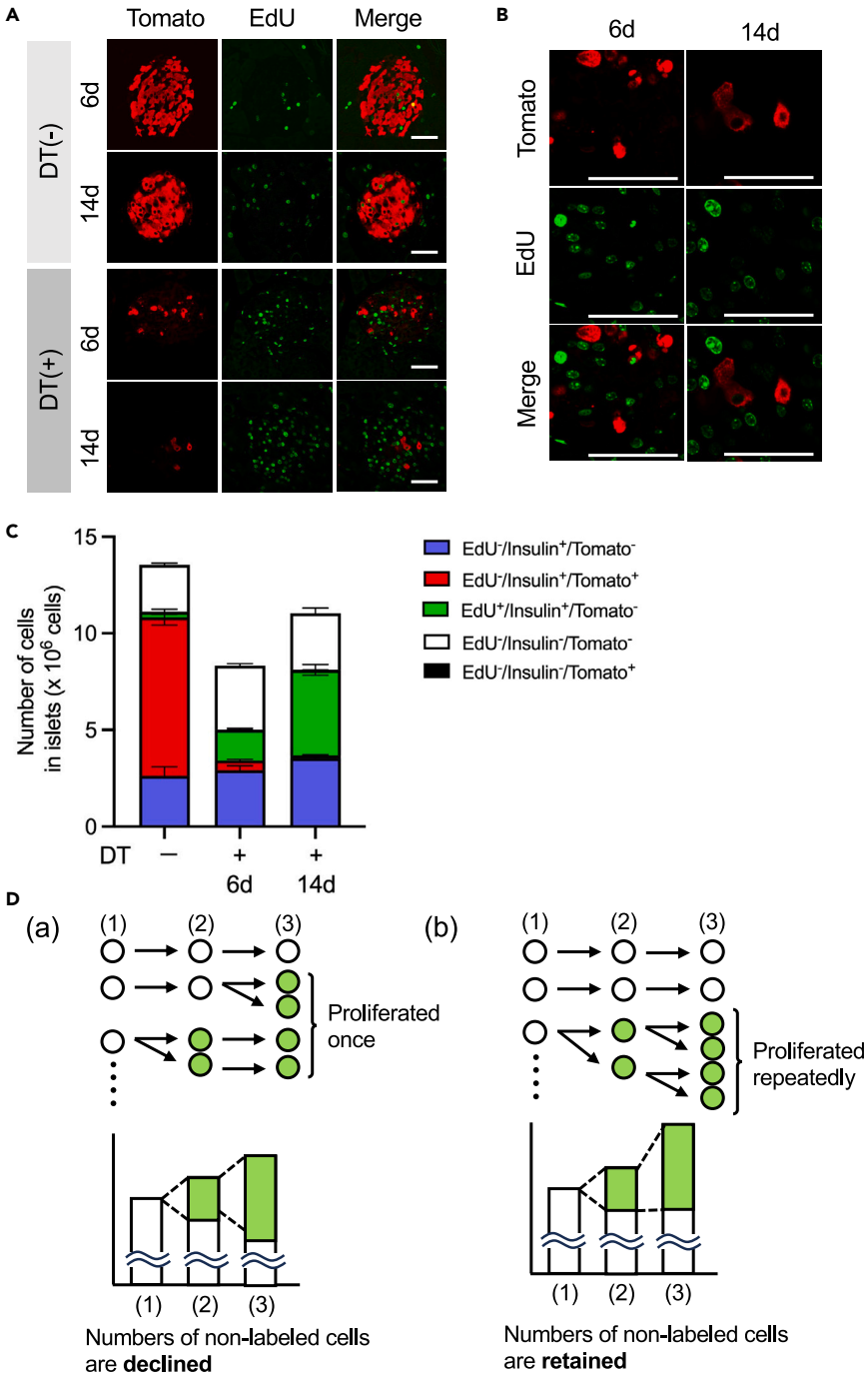

Figure 2. Visualization and quantification of β cell proliferation in DT-treated DTR mice

(A and B) (A) Pancreatic islets from PBS- and DT-treated mice co-stained with tdTomato and EdU. Magnified image of Tomato/EdU co-staining in DT-treated DTR mice in (B). Scale bars: 50 μm.

(C) Calculated number of insulin-positive cells, tomato-positive, and EdU-positive cells. Data are expressed as mean ± SEM. DT(−)+6 days: $n = 3$, DT(−)+14 days: $n = 3$, DT+6 days: $n = 6$, DT+14 days: $n = 6$, respectively.

(D) Schematic models for different modes of β cell proliferation. (a) sporadic β cell proliferation; (b) repeated β cell proliferation. Green, EdU-positive β cells.

of MafA^{+ve}/Ins^{+ve} cells was restored 14 days after DT treatment (Figure S5). Interestingly, the ratio of MafA^{+ve} cell number to Ins^{+ve} cell number was positively correlated with the change in mean cell size (Figure S5C). These results indicate that small, immature (MafA^{-ve}) β cells were increased during β cell proliferation after DT treatment.

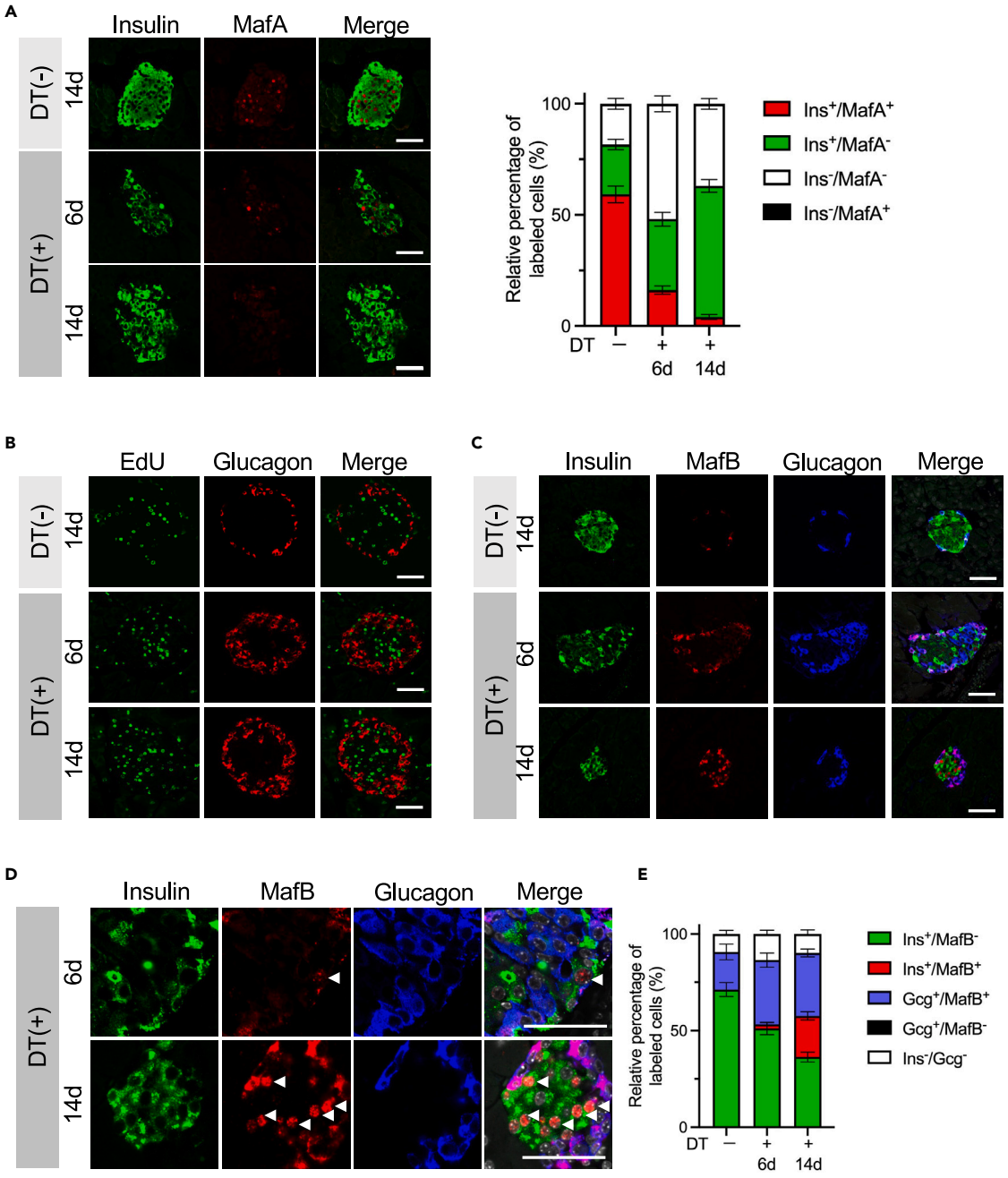

Figure 3. Immunohistochemical analyses of cellular properties of β cells in DT-treated DTR mice

(A) Representative images of co-immunostaining of MafA and insulin in control [DT(–): PBS-treated for 14 days], and DT-treated DTR mice (6 and 14 days). The percentages of labeled cells are displayed by bar plot. Data are expressed as mean ± SEM.

(B) Representative images of co-immunostaining of EdU and glucagon, in control [DT(–): PBS-treated for 14 days], and DT-treated DTR mice (6 and 14 days).

(C–E) Representative images of co-immunostaining of Insulin, MafB, and glucagon in control [DT(–): PBS-treated for 14 days], and DT-treated DTR mice (6 and 14 days) (higher magnification shown in (D). Scale bars: 50 μm. The percentages of labeled cells shown in (C) are displayed by bar plot in (E). Data are expressed as mean ± SEM.

In contrast, MafB, a generally accepted marker of immature β cells, was only sparsely detected in cells at the periphery of the islets of DT-untreated DTR mice. These MafB-positive ($MafB^{+ve}$) cells also stained positive for glucagon (Figure 3B), indicating that they are α-cells rather than immature β cells. In contrast, the number of $MafB^{+ve}$ cells in the islets of DTR mice was increased 6 days after DT administration (Figures 3C and 3D). Importantly, EdU was not incorporated into glucagon-positive α-cells after DT administration in DTR mice (Figure 3B),

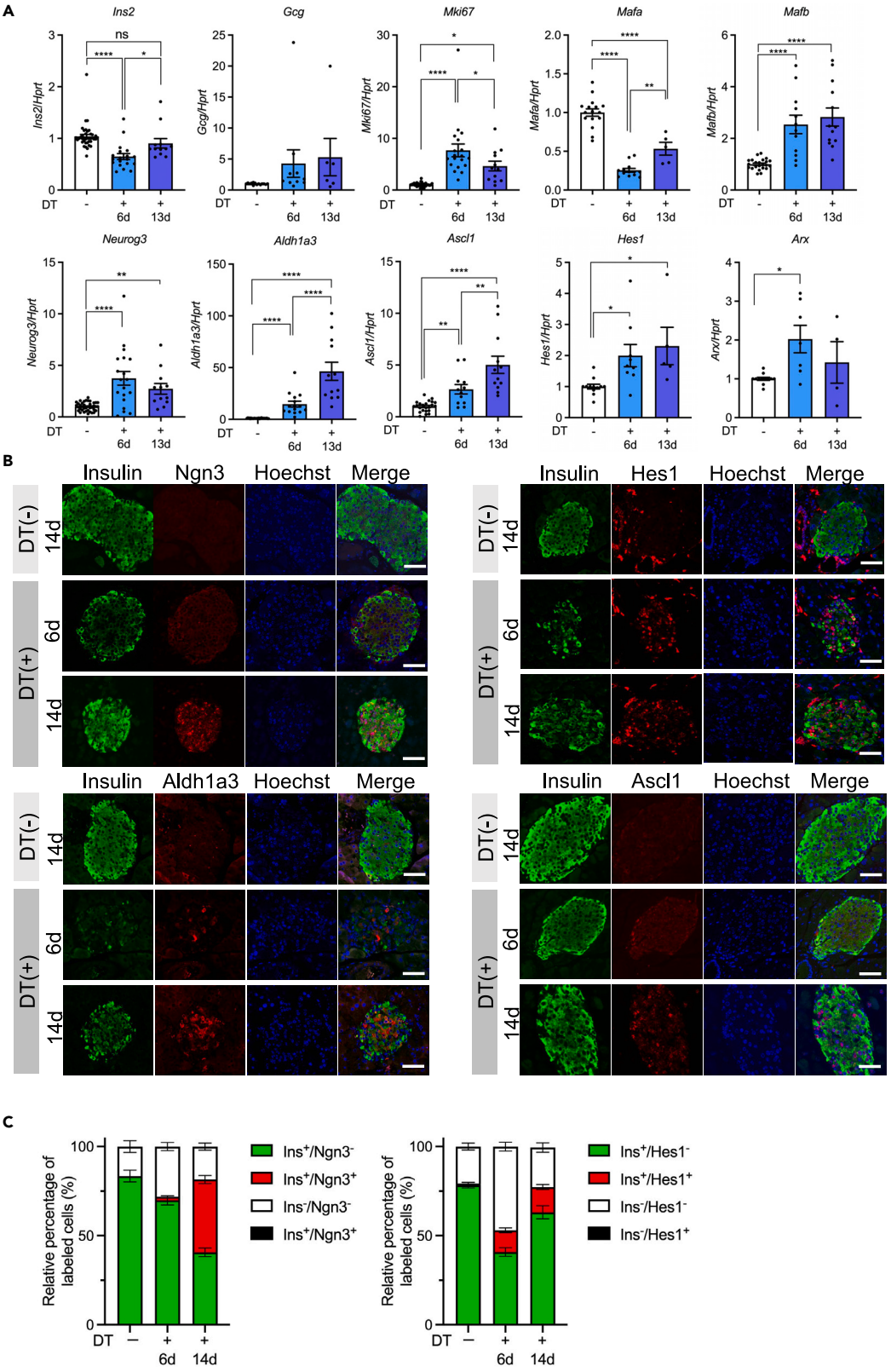
A
Ins2
Gcg
Mki67
Mafa
Mafb
Neurog3
Aldh1a3
Ascl1
Hes1
Arx
Ins2/Hprt
Gcg/Hprt
Mki67/Hprt
Mafa/Hprt
Mafb/Hprt
Neurog3/Hprt
Aldh1a3/Hprt
Ascl1/Hprt
Hes1/Hprt
Arx/Hprt
ns
DT
6d
13d
B
Insulin
Ngn3
Hoechst
Merge
Hes1
Aldh1a3
Ascl1
DT(-)
DT(+)
14d
6d
C
Relative percentage of labeled cells (%)
Ins+/Ngn3-
Ins+/Ngn3+
Ins-/Ngn3-
Ins+/Ngn3+
Ins+/Hes1-
Ins+/Hes1+
Ins-/Hes1-
Ins-/Hes1+

Figure 4. mRNA expression of genes involved in cellular function of endocrine pancreas and immunostaining of Aldh1a3 in islets of DT-administered DTR mice

(A) Expression levels of mature β cell markers (*Ins2* and *Mafa*), a proliferating cell marker (*Mki67*), immature β cell markers (*Neurog3* and *Mafb*), and mature α cell markers (*Gcg*, and *Arx*) in control (DT(−): PBS-treated for 13 days: $n = 12\sim22$) and DT-treated DTR mice (6 and 14 days) ($n = 7\sim19$ and $n = 5\sim12$, respectively). Data are expressed as mean ± SEM. ****$p < 0.0001$, ***$p < 0.001$, **$p < 0.01$, *$p < 0.05$.

(B) Representative images of co-immunostaining (immature β cell markers [Ngn3, Aldh1a3, Hes1, or Ascl1] and insulin) in control (DT(−): PBS-treated for 14 days) and DT-treated DTR mice (6 and 14 days). Scale bars: 50 μm.

(C) The percentages of $Ngn3^{+ve}$ or $Hes1^{+ve}$ cells are displayed by bar plot. Data are expressed as mean ± SEM.

while $MafB^{+ve}$ cells in the islets were increased in number after DT administration, and most of them stained negative for glucagon (Figures 3C and 3D) but weakly positive for insulin (Figures 3C and 3D). Thus, $MafB^{+ve}$ cells after DT administration are immature β cells. As Gcg^{+ve} cells comprised most of the Ins^{-} cells (Figure 3E), Ins^{-ve}/Gcg^{-ve} cells were further examined. δ-cells, the second highest population among non-β cells, were immunostained with somatostatin (Sst) antibody, but no increase in Sst^{+ve} cells during regeneration was noted (Figure S6).

We then quantified the mRNA expression of immature β cell markers in the islets using laser-captured microdissection (LCM). Consistently with the immunostaining findings, the mRNA expression of the markers of mature β cells (*Ins2* and *Mafa*) were decreased (Figure 4A). Concurrently, both a proliferation marker (*Mki67*) and an immature β cell marker (*Mafb*) were increased. On day 6 and 13 after DT treatment, mRNA expression of the α-cell markers (*Gcg* and *Arx*) was increased. However, the number of α-cells was not increased, suggesting that the higher *Gcg*, *Arx*, and *Mafb* levels may be due to the relative increase in α-cell number together with the massive decrease in β cell number. We then examined the expression of other markers for immature β cells including hairy and enhancer of split-1 (*Hes1*), neurogenin-3 (*Neurog3*), and *Aldh1a3*, a dedifferentiated β cell marker. These genes were increased after β cell ablation by DT but with a differing dynamic, *Neurog3* peaking on day 6, *Hes1* and *Aldh1a3* continuing to day 13. *Ascl1*, one of transcriptional regulators of *Aldh1a3*, also increases along with *Aldh1a3* expression. Immunoreactivity of neurogenin 3 (Ngn3) was predominantly detected in the cytoplasmic area on day 6, but its nuclear localization became distinct on day 14 (Figures 4B and 4C). On the other hand, nuclear localization of Hes1 was found both on day 6 and day 14 (Figures 4B and 4C). Ascl1 and Aldh1a3 expression were weak on day 6 but were markedly increased on day 14 (Figure 4B). Accordingly, β cell dedifferentiation, manifested by increased Ngn3, Hes1, Ascl1, and Aldh1a3, is likely to have reduced MafA, which may well coincide with the proliferation process in these mice considering that each these factors represents a distinct and specific stage of regeneration.

β cells maintained their maturity during active regeneration induced by partial pancreatectomy

We then performed the same analyses in PPx mice. The number of EdU^{+ve} β cells was found to be increased in response to ∼70% partial pancreatectomy along with an increase in the number of EdU^{+ve} exocrine cells (Figure 5A)., $Ki67^{+ve}$ cells in PPx mice were only sparsely observed until day 6, as was the case in DTR mice (Figure S2). Induction of cell proliferation by PPx was similar to that in DTR mice as assessed by EdU incorporation both on day 6 and 14 (Figure 5A). In contrast to DTR mice, mean cell size was not altered in PPx mice (Figure 5B). In addition, immunoreactivity of insulin and MafA in EdU^{+ve} β cells was not decreased after PPx (Figure 5C). Although *Mki67* mRNA expression was increased by PPx to similar level to that in DTR mice, mRNA expression of mature β cell marker genes (*Ins2* and *Mafa*) was only mildly decreased. Interestingly, immature β cell marker gene expression (*Mafb*, *Hes1*, and *Neurog3*) was not increased. In addition, *Ascl1* and *Aldh1a3* expressions were mildly increased at the mRNA level (Figure 5D). Immunostaining also showed no apparent upregulation of immature β cell markers (Ngn3, Hes1, Ascl1, and Aldh1a3) (Figure 5E) and continuous nuclear localization of MafA (Figure 5C), suggesting that PPx triggers β cell proliferation without inducing dedifferentiation. Even in the early stages (up to day 6), no apparent expression of immature β cell markers was detected in PPx mice.

A small subset of the residual β cells underwent repeated proliferation in DT-administered DTR mice

The lack of decrease in EdU^{-ve} β cells during regeneration in DT-administered DTR mice (Figure 2C) suggested that only a small number of the residual β cells were induced to repeated proliferation (Figure 2D, *right*). We therefore performed sequential labeling using two, different nucleoside analogs, EdU and BrdU, in both DT-administered DTR and PPx mice, as shown in Figure 6A. In both models, a similar number of β cells stained positive for EdU and BrdU (Figures 6B and 6C). However, $EdU^{+ve}/BrdU^{+ve}$ β cells were detected more frequently in DTR mice (approximately 33.1 ± 0.8% of $BrdU^{+ve}$ β cells) than in PPx mice (approximately 6.6 ± 1.8%. $p < 0.001$), suggesting highly proliferative immature β cells in DT-administered DTR islets.

To characterize the proliferating β cells in DT-administered DTR mice, co-immunostaining of Ki67 with immature β cell markers (Ngn3, Hes1, Ascl1, and Aldh1a3) was conducted 14 days after treatment. As shown in Figure 7A, $Ki67^{+ve}$ proliferating cells are evident in Ngn3- and Hes1-positive β cells but not in Aldh1a3-, Ascl1-, or MafA-positive β cells, suggesting that β cell proliferation occurs readily in premature Ngn3-and Hes1-positive β cells. Interestingly, in islets sequentially labeled with EdU/BrdU, Aldh1a3 immunoreactivity was higher in EdU single-positive β cells than those in BrdU single positive β cells or EdU/BrdU double-positive β cells (Figure 7B), implying that Aldh1a3 expression is induced late after proliferation. These findings suggest that induction of Hes1/Ngn3 is induced first in residual β cells during repeated proliferation.

We then addressed the regulatory mechanism of Hes1 and Ngn3 induction in the residual β cells. Crosstalk between these two bHLH family members is known to regulate neural development. These protein expressions are oscillatory and effected through negative-feedback

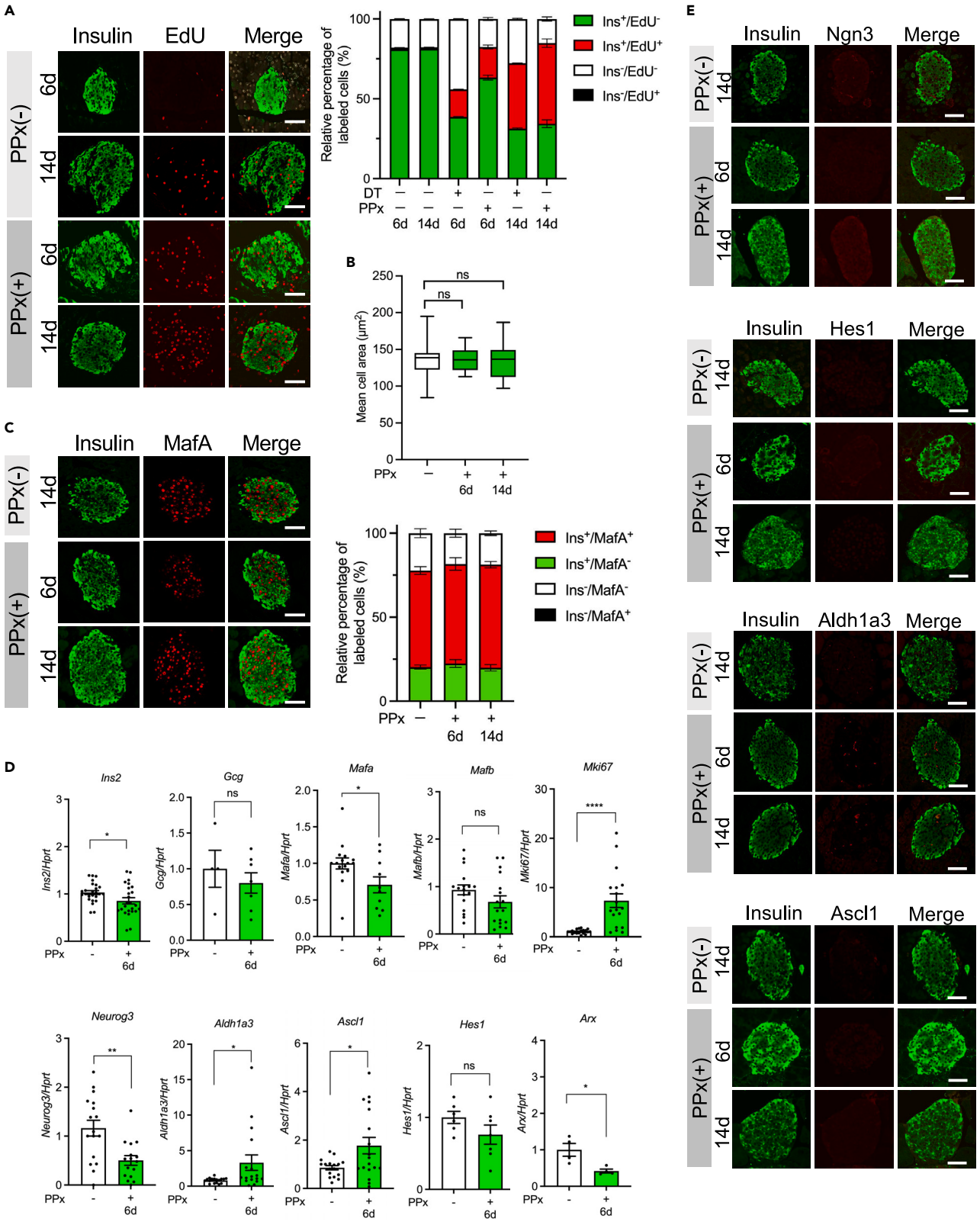
A
Insulin
EdU
Merge
PPx(-)
PPx(+)
6d
14d
Relative percentage of labeled cells (%)
Ins+/EdU-
Ins+/EdU+
Ins-/EdU-
Ins-/EdU+
DT
PPx
B
Mean cell area (μm2)
ns
C
Insulin
MafA
Merge
Relative percentage of labeled cells (%)
Ins+/MafA+
Ins+/MafA-
Ins-/MafA-
Ins-/MafA+
D
Ins2
Gcg
Mafa
Mafb
Mki67
Neurog3
Aldh1a3
Ascl1
Hes1
Arx
E
Insulin
Ngn3
Merge
Hes1
Aldh1a3
Ascl1

Figure 5. Immunostaining and RT-qPCR analysis of genes involved in islet regeneration in PPx mice

(A) Pancreatic islets from sham (day 6 and 14) and PPx mice (day 6 and 14) co-stained with insulin and EdU. Relative percentages of labeled cells are displayed by bar plot. Data are expressed as mean ± SEM.

(B) Mean cell size of islets. Data are expressed as mean ± SEM.

(C) Co-immunostaining of insulin and MafA in PPx mice.

(D) Expression levels of mature β cell markers (*Ins2* and *Mafa*), a proliferating cell marker (*Mki67*), immature β cell markers (*Neurog3* and *Mafb*), and mature α cell markers (*Gcg* and *Arx*) in Sham (6 days: n = 4∼17) and PPx mice (n = 4–24). Data are expressed as mean ± SEM. ****$p < 0.0001$, **$p < 0.01$, *$p < 0.05$.

(E) Co-immunostaining [immature β cell markers (Ngn3, Aldh1a3, Hes1, or Ascl1) with insulin] in PPx mice. Scale bars: 50 μm.

autoregulation of Hes1.[22] We then examined the fibroblast growth factor (FGF) signaling pathway, which is involved in transactivation of *Hes1*.[22,23] Intriguingly, we found that *Fgf2* expression was significantly upregulated in DT-administered DTR mice but not in PPx mice (Figure 7C), implying that *Hes1* upregulation is triggered through FGF signaling in these mice.

β cell ablation rather than increased insulin secretory needs triggered proliferation in DT-administered DTR mice

DT-administered induction of comparable β cell proliferation in response to the similar degree of β cell loss in DT-administered DTR and PPx mice indicates that the β cell decreases in both models were sufficient to trigger proliferation. To confirm this, we endowed the PPx mice with excess β cells by sub-renal transplantation (SRT) of pseudo-islets of mouse insulinoma MIN6 cells prior to PPx (Figure 8A), and PPx-induced β cell proliferation was markedly attenuated by this transplantation (Figure 8B). While SRT also suppressed DT-induced β cell proliferation in DTR mice, the suppression was much less than that in PPx mice (Figure 8C), suggesting that mosaic DT-induced β cell ablation in DTR mice can trigger β cell proliferation in the absence of increased insulin secretory need.

In SRT(+) DTR mice, the number of EdU^{+ve} β cells was reduced to about one-third of that in SRT(−) DTR mice (Figure 8D). This value roughly matches the rate of $EdU^{+ve}/BrdU^{+ve}$ β cells shown in Figures 6B and 6C. These findings suggest that the increased need for additional insulin secretion due to PPx triggers random β cell proliferation while DT-induced β cell ablation in DTR mice triggers progenitor-like β cell proliferation.

DISCUSSION

Our examination of genetic ablation of β cells in DTR mice reveals that a small subset of differentiated β cells in adult mice can be induced to proliferate repeatedly through a dedifferentiation/proliferation/redifferentiation process. In contrast, in our examination of surgical reduction of β cell mass by PPx, the number of functional β cells was reduced to a degree similar to the DT-administered DTR mice and resulted in a similar degree of proliferation but in a mode of replication not including dedifferentiation. These findings demonstrate that β cell regeneration can be triggered not only by increased requirement for insulin but also by variation in the microenvironment of the residual cells.

Zhao et al. previously reported that pre-existing β cells but not β cell progenitors replenish β cell mass in several adult mouse models of regeneration including PPx, pregnancy, PDL, and STZ-treated mice.[24] They demonstrated that proliferating β cells are positive for lineage-tracing markers of β cells but not those of non-β cell markers, seeming to exclude the possibilities of proliferation/differentiation of stem/progenitor cells into β cells (neogenesis) and *trans*-differentiation of non-β endocrine pancreas into β cells. However, extreme ablation (∼99%) of β cells in RIP-DT mice has been shown to induce β cell regeneration by *trans*-differentiation from non-β cells without proliferation of residual β cells.[16,17] In the present study, we demonstrate that proliferation of pre-existing β cells but not *trans*-differentiation of non-β cells to β cells occurs in islet regeneration in approximately 80% β cell-ablated DT-administered DTR mice. Interestingly, a small subset of β cells was found to proliferate repeatedly in tandem with an increase in islet expression of premature β cell marker genes including MafB, Hes1, Ngn3, Ascl1, and Aldh1a3 and a decrease in cell size and MafA expression, which is not seen in PPx mice, indicating that de-differentiation of pre-existing β cells is involved in our model of islet regeneration in DT-administered DTR mice.

It is now widely accepted that de-differentiation of β cells is an underlying mechanism in T2DM onset and that upregulation of β cell-disallowed genes (such as *Ngn3* and *Aldh1a3*) might be the hallmark of β cell de-differentiation.[25–27] However, our results imply that, as well as being markers of β cell dysfunction, Ngn3 and Aldh1a3 also mark a regenerative process involving de-differentiation and repeated bursts of proliferation. Thus, de-differentiation may be an adaptive response to avoid cell death from pathological conditions induced by oxidative stress, endoplasmic reticulum (ER) stress, and inflammatory cytokines. Indeed, acquisition of endocrine progenitor-like features is thought to be beneficial for their replication.

Among the various potential accelerators of β cell dedifferentiation, activation of Notch signaling in mature β cells has been reported to obliterate their maturity but provide Notch-active β cells with proliferative capacity through activation of Hes1, a Notch effector transcription regulator.[28–30] Notch activity is known to be regulated by neighboring cells through cell-to-cell binding of the ligands and receptors involved in Notch signaling.[20,21] On the other hand, Hes1 expression is also regulated by the FGF signaling pathway. FGF also contributes to maintain the stemness of neural progenitor cells by transactivation of Hes1 through Ras/ERK signaling.[23] In this study, mosaic DT-induced β cell ablation may well have resulted in loss of cell-to-cell contact between neighboring β cells and loss of cell-to extracellular matrix (ECM) contact. Saunders et al. recently reported that maintaining islet microenvironments by coordinated interactions among endothelial cells, macrophages, ECM, and β cells are important for the regeneration of β cells.[31] Diedisheim et al. report that FGF2 treatment induces human β cell dedifferentiation and upregulates gene expression of FGF2 and its receptor FGFR1 along with HES1 transactivation in human T2DM patients.[32] They find that FGF2 is transactivated in pancreatic stellate cells, endothelial cells,

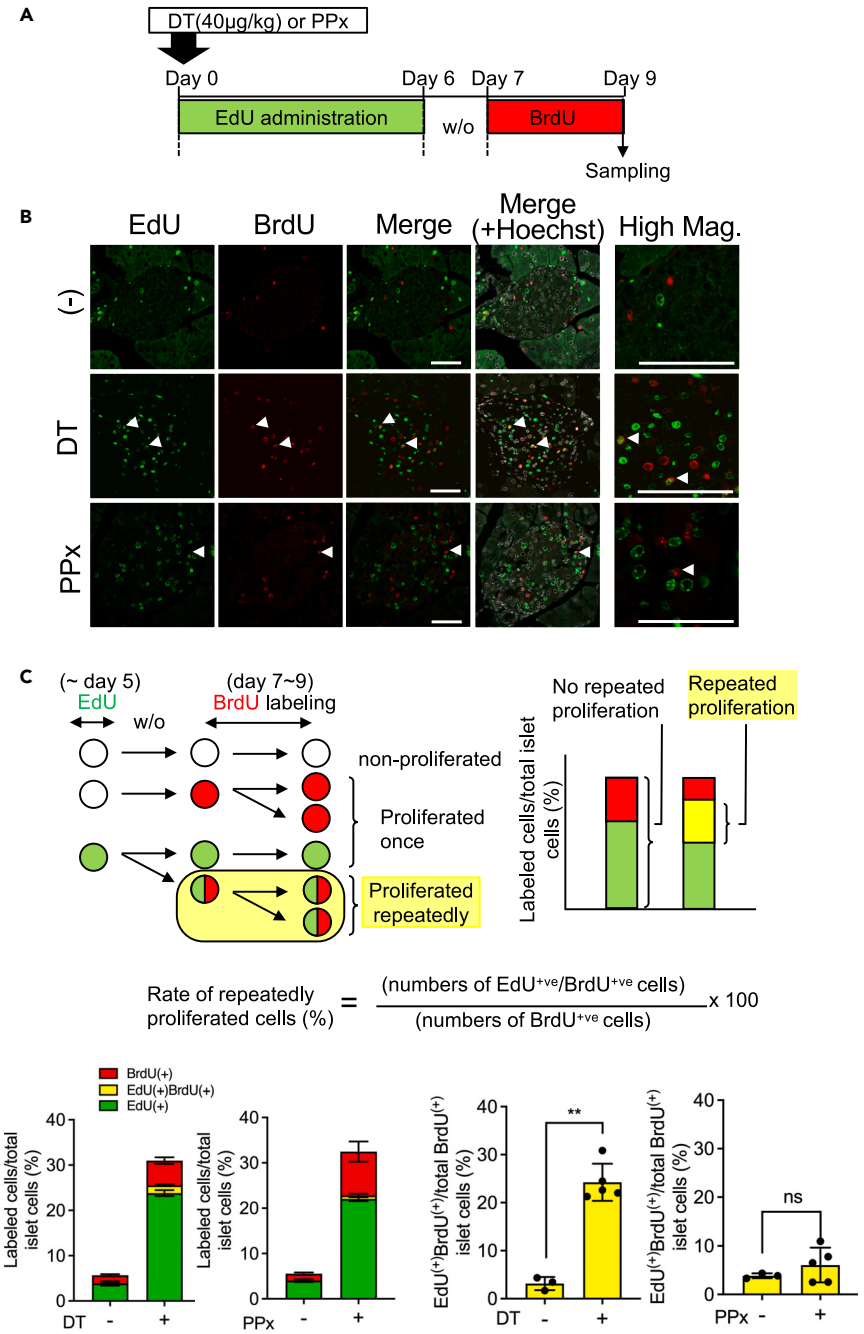

Figure 6. Dual labeling of proliferating cells by EdU and BrdU in DT-treated DTR and PPx mice

(A) Protocol of dual labeling (EdU and BrdU) of proliferating cells in DTR and PPx mice.

(B) Representative images of co-staining (EdU and BrdU) in control (PBS), DTR, and PPx mice. *Arrowhead*: $EdU^+/BrdU^+$ cells. Scale bars: 50 μm.

(C) A schematic model for dual consecutive labeling of proliferating β cells (top). Numbers of EdU^+, $BrdU^+$, $EdU^+/BrdU^+$ cells in islets (middle) and the ratio of labeled cells (bottom) per total number of islet cells ($Hoechst^+$). [DT(−): $n = 3$, DT(+): $n = 5$, PPx(−): $n = 5$, PPx(+): $n = 5$]. $^{**}p < 0.01$.

and ductal cells. FGF2 (also known as bFGF) is known to play an important role in wound healing, tissue regeneration, and angiogenesis.[33] In this context, disrupted cell-to-cell or cell-to-ECM interaction may stimulate those cells to secrete FGF2 for reconstruction of islet microenvironments.

We conclude that β cell regeneration occurs in at least two distinct modes in mice. Increased insulin demand elicits pre-existing β cell replication without dedifferentiation, by which the structural integrity of the β cell is maintained. However, when cell-to-cell or cell-to-ECM

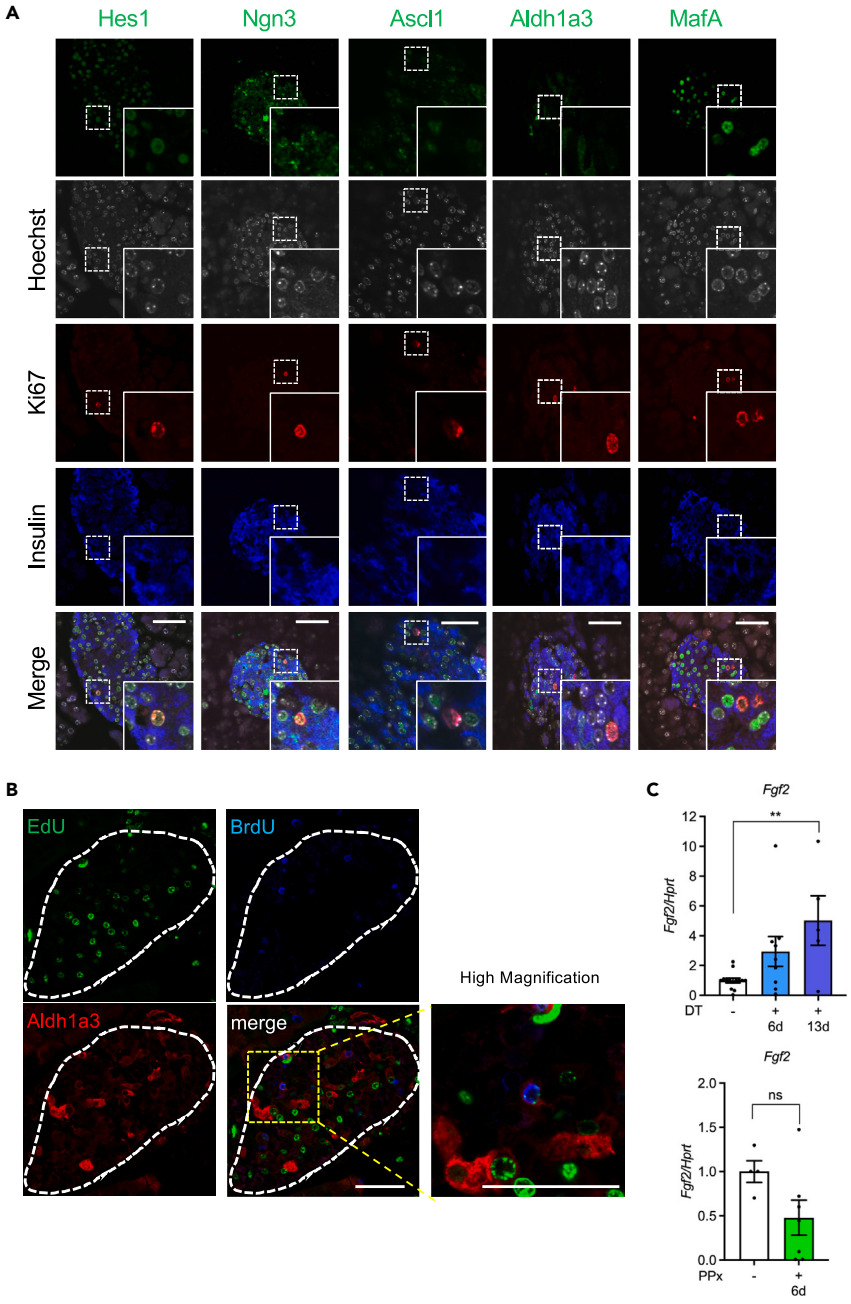

Figure 7. Characterization of proliferating β cells in DTR mice

(A) Triple immunostaining for immature (Hes1, Ngn3, Ascl1, or Aldh1a3) or mature (MafA) β cell marker with insulin and Ki67 in DT-treated DTR mice (day 6).

(B) Co-immunostaining of Aldh1a3 with EdU/BrdU in DTR mice (day 9). Scale bars: 50 μm.

(C) Expression levels of *Fgf2* in control (DT(−): PBS-treated for 14 days: $n = 12$) and DT-treated DTR mice (6 and 13 days) ($n = 9$ and $n = 5$, respectively) and in Sham ($n = 4$) and PPx mice ($n = 7$). Data are expressed as mean ± SEM. $^{**}p < 0.01$.

interaction among β cells is disrupted by, for example, mosaic ablation of β cells in DT-administered DTR mice, de-differentiation of the residual β cells may be triggered and a small subset of these cells elicit progenitor-like, repetitive proliferation of pre-existing β cells followed by redifferentiation into mature β cells. Our finding that a small fraction of differentiated β cells in adult mice can undergo repeated proliferation to replenish β cell mass has not been previously reported. This study provides a rationale for pursuing a radical strategy against T2DM of promotion of β cell regeneration, although further study is required to ascertain whether repeated proliferation of a small fraction of β cells can be induced in aged, human patients with T2DM.

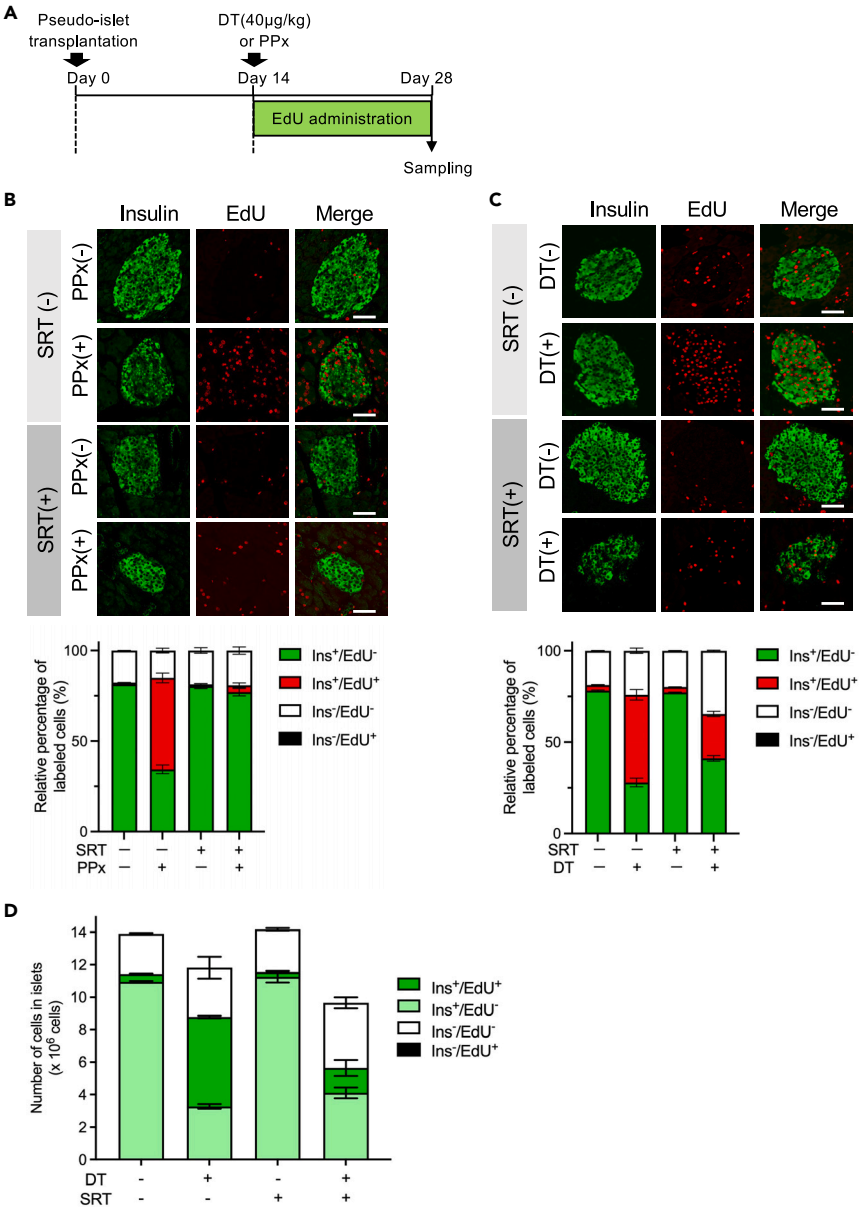

Figure 8. Effect of pseudo-islet transplantation on β cell regeneration in DT-treated DTR and PPx mice

(A) Protocol of pseudo-islet transplantation and EdU labeling in DTR and PPx mice. Representative images of co-immunostaining.

(B) Insulin and EdU in DTR mice with and without SRT. Relative percentages of labeled cells are displayed by bar plot. Data are expressed as mean ± SEM.

(C) Representative image of co-staining (Insulin and EdU) in PPx mice with and without SRT. Scale bars: 50 μm. Relative percentages of labeled cells are displayed by bar plot. Data are expressed as mean ± SEM.

(D) Calculated number of cells in DTR mice and PPx mice with and without SRT. Data are expressed as mean ± SEM. DT(−)/SRT(−): $n = 4$, DT(+)/SRT(−): $n = 3$, DT(−)/SRT(+): $n = 3$, DT(+)/SRT(+): $n = 4$ respectively. Data are expressed as mean ± SEM.

Limitations of the study

Although we suggest that dedifferentiation of β cells in the DT-administered DTR mice is can be attributed to features of an islet microenvironment, the molecular mechanism remains unclear. In addition, we were unable to verify the temporal expressions of bHLH factors including Hes1, Ngn3, and Ascl1 during β cell regeneration. Future, single cell transcriptomic analysis would help clarify the temporal regulatory mechanism of β cell regeneration.

RESOURCE AVAILABILITY

Lead contact

Further information and requests for resources and reagents should be directed to and will be fulfilled by the lead contact, Ryo Hatano (hatanori@chiba-u.jp).

Materials availability

This study did not generate new unique reagents and materials.

Data and code availability

Data reported in this paper will be shared by the lead contact upon request. This paper does not report original code. Any additional information required to reanalyze the data reported in this paper is available from the lead contact upon request.

ACKNOWLEDGMENTS

The authors acknowledge Dr. Kenichi Sakurai for helpful discussion. This research was supported by JSPS KAKENHI (grant numbers: JP23K06343 for R.H., JP24K10023 for E.Y.L., and JP19K07281 and JP23K24062 for T.M.).

AUTHOR CONTRIBUTIONS

Conceptualization, R.H. and T.M.; investigation, R.H., X. Z., and E.Y.L.; data curation, R.H., X. Z., and E.Y.L.; methodology, R.H., X. Z., E.Y.L, and A.K., validation, R.H., and E.Y.L.; visualization, R.H. and X.Z.; resources, A.K. and T.T.; formal analysis, R.H. and X.Z.; supervision, A.K., T.T., and T.M.; project administration, M.T.; funding acquisition, R.H. , E.Y.L., and M.T.; writing – original draft, R.H. and T.M.; writing – review and editing, R.H. and T.M.

DECLARATION OF INTERESTS

The authors declare no competing interest.

STAR★METHODS

Detailed methods are provided in the online version of this paper and include the following:

- KEY RESOURCES TABLE
- EXPERIMENTAL MODEL AND STUDY PARTICIPANT DETAILS
  - Animals
- METHOD DETAILS
  - Antibodies
  - Animal models
  - Labeling of proliferating cells
  - Preparation of pseudo-islets and transplantation
  - Histological analysis
  - Laser capture microdissection of islets
- QUANTIFICATION AND STATISTICAL ANALYSIS

SUPPLEMENTAL INFORMATION

Supplemental information can be found online at https://doi.org/10.1016/j.isci.2024.110656.

Received: March 18, 2024
Revised: June 27, 2024
Accepted: July 31, 2024
Published: August 3, 2024

REFERENCES

1. Lee, E.Y., Sakurai, K., Zhang, X., Toda, C., Tanaka, T., Jiang, M., Shirasawa, T., Tachibana, K., Yokote, K., Vidal-Puig, A., et al. (2015). Unsuppressed lipolysis in adipocytes is linked with enhanced gluconeogenesis and altered bile acid physiology in Insr$^{(P1195L/+)}$ mice fed high-fat-diet. Sci. Rep. *5*, 17565. https://doi.org/10.1038/srep17565.
2. Butler, A.E., Janson, J., Bonner-Weir, S., Ritzel, R., Rizza, R.A., and Butler, P.C. (2003). Beta-cell deficit and increased beta-cell apoptosis in humans with type 2 diabetes. Diabetes *52*, 102–110. https://doi.org/10.2337/diabetes.52.1.102.
3. Padhi, S., Nayak, A.K., and Behera, A. (2020). Type II diabetes mellitus: a review on recent drug-based therapeutics. Biomed. Pharmacother. *131*, 110708. https://doi.org/10.1016/j.biopha.2020.110708.
4. Sasaki, S., Lee, M.Y.Y., Wakabayashi, Y., Suzuki, L., Winata, H., Himuro, M., Matsuoka, T.A., Shimomura, I., Watada, H., Lynn, F.C., and Miyatsuka, T. (2022). Spatial and transcriptional heterogeneity of pancreatic beta cell neogenesis revealed by a time-resolved reporter system. Diabetologia *65*, 811–828. https://doi.org/10.1007/s00125-022-05662-0.
5. Ernst, S., Demirci, C., Valle, S., Velazquez-Garcia, S., and Garcia-Ocaña, A. (2011). Mechanisms in the adaptation of maternal β cells during pregnancy. Diabetes Manag. *1*, 239–248. https://doi.org/10.2217/dmt.10.24.
6. Ying, W., Lee, Y.S., Dong, Y., Seidman, J.S., Yang, M., Isaac, R., Seo, J.B., Yang, B.H., Wollam, J., Riopel, M., et al. (2019). Expansion of Islet-Resident Macrophages Leads to Inflammation Affecting β Cell Proliferation and Function in Obesity. Cell Metabol. *29*, 457–474.e5. https://doi.org/10.1016/j.cmet.2018.12.003.
7. Saunders, D., and Powers, A.C. (2016). Replicative capacity of β-cells and type 1 diabetes. J. Autoimmun. *71*, 59–68. https://doi.org/10.1016/j.jaut.2016.03.014.
8. Aguayo-Mazzucato, C., and Bonner-Weir, S. (2018). Pancreatic β Cell Regeneration as a

Possible Therapy for Diabetes. Cell Metabol. *27*, 57–67. https://doi.org/10.1016/j.cmet.2017.08.007.

9. Dor, Y., Brown, J., Martinez, O.I., and Melton, D.A. (2004). Adult pancreatic beta-cells are formed by self-duplication rather than stem-cell differentiation. Nature *429*, 41–46. https://doi.org/10.1038/nature02520.
10. Xu, X., D'Hoker, J., Stangé, G., Bonné, S., De Leu, N., Xiao, X., Van de Casteele, M., Mellitzer, G., Ling, Z., Pipeleers, D., et al. (2008). Beta cells can be generated from endogenous progenitors in injured adult mouse pancreas. Cell *132*, 197–207. https://doi.org/10.1016/j.cell.2007.12.015.
11. Inada, A., Nienaber, C., Katsuta, H., Fujitani, Y., Levine, J., Morita, R., Sharma, A., and Bonner-Weir, S. (2008). Carbonic anhydrase II-positive pancreatic cells are progenitors for both endocrine and exocrine pancreas after birth. Proc. Natl. Acad. Sci. USA *105*, 19915–19919. https://doi.org/10.1073/pnas.0805803105.
12. Lee, C.S., De León, D.D., Kaestner, K.H., and Stoffers, D.A. (2006). Regeneration of pancreatic islets after partial pancreatectomy in mice does not involve the reactivation of neurogenin-3. Diabetes *55*, 269–272.
13. Tschen, S.I., Dhawan, S., Gurlo, T., and Bhushan, A. (2009). Age-dependent decline in beta-cell proliferation restricts the capacity of beta-cell regeneration in mice. Diabetes *58*, 1312–1320. https://doi.org/10.2337/db08-1651.
14. Rankin, M.M., and Kushner, J.A. (2009). Adaptive beta-cell proliferation is severely restricted with advanced age. Diabetes *58*, 1365–1372. https://doi.org/10.2337/db08-1198.
15. Zhong, F., and Jiang, Y. (2019). Endogenous Pancreatic β Cell Regeneration: A Potential Strategy for the Recovery of β Cell Deficiency in Diabetes. Front. Endocrinol. *10*, 101. https://doi.org/10.3389/fendo.2019.00101.
16. Thorel, F., Népote, V., Avril, I., Kohno, K., Desgraz, R., Chera, S., and Herrera, P.L. (2010). Conversion of adult pancreatic α-cells to β-cells after extreme beta-cell loss. Nature *464*, 1149–1154. https://doi.org/10.1038/nature08894.
17. Chera, S., Baronnier, D., Ghila, L., Cigliola, V., Jensen, J.N., Gu, G., Furuyama, K., Thorel, F., Gribble, F.M., Reimann, F., and Herrera, P.L. (2014). Diabetes recovery by age-dependent conversion of pancreatic δ-cells into insulin producers. Nature *514*, 503–507. https://doi.org/10.1038/nature13633.
18. Postic, C., Shiota, M., Niswender, K.D., Jetton, T.L., Chen, Y., Moates, J.M., Shelton, K.D., Lindner, J., Cherrington, A.D., and Magnuson, M.A. (1999). Dual roles for glucokinase in glucose homeostasis as determined by liver and pancreatic beta cell-specific gene knock-outs using Cre recombinase. J. Biol. Chem. *274*, 305–315. https://doi.org/10.1074/jbc.274.1.305.
19. Morita, A., Mukai, E., Hiratsuka, A., Takatani, T., Iwanaga, T., Lee, E.Y., and Miki, T. (2016). Distinct effects of dipeptidyl peptidase-4 inhibitor and glucagon-like peptide-1 receptor agonist on islet morphology and function. Endocrine *51*, 429–439. https://doi.org/10.1007/s12020-015-0733-4.
20. Chacón-Martínez, C.A., Koester, J., and Wickström, S.A. (2018). Signaling in the stem cell niche: regulating cell fate, function and plasticity. Development *145*, dev165399. https://doi.org/10.1242/dev.165399.
21. Hicks, M.R., and Pyle, A.D. (2023). The emergence of the stem cell niche. Trends Cell Biol. *33*, 112–123. https://doi.org/10.1016/j.tcb.2022.07.003.
22. Dhanesh, S.B., Subashini, C., and James, J. (2016). Hes1: the maestro in neurogenesis. Cell. Mol. Life Sci. *73*, 4019–4042. https://doi.org/10.1007/s00018-016-2277-z.
23. Nakayama, K., Satoh, T., Igari, A., Kageyama, R., and Nishida, E. (2008). FGF induces oscillations of Hes1 expression and Ras/ERK activation. Curr. Biol. *18*, R332–R334. https://doi.org/10.1016/j.cub.2008.03.013.
24. Zhao, H., Huang, X., Liu, Z., Pu, W., Lv, Z., He, L., Li, Y., Zhou, Q., Lui, K.O., and Zhou, B. (2021). Pre-existing beta cells but not progenitors contribute to new beta cells in the adult pancreas. Nat. Metab. *3*, 352–365. https://doi.org/10.1038/s42255-021-00364-0.
25. Talchai, C., Xuan, S., Lin, H.V., Sussel, L., and Accili, D. (2012). Pancreatic β cell dedifferentiation as a mechanism of diabetic β cell failure. Cell *150*, 1223–1234. https://doi.org/10.1016/j.cell.2012.07.029.
26. Cinti, F., Bouchi, R., Kim-Muller, J.Y., Ohmura, Y., Sandoval, P.R., Masini, M., Marselli, L., Suleiman, M., Ratner, L.E., Marchetti, P., and Accili, D. (2016). Evidence of β-Cell Dedifferentiation in Human Type 2 Diabetes. J. Clin. Endocrinol. Metab. *101*, 1044–1054. https://doi.org/10.1210/jc.2015-2860.
27. Kim-Muller, J.Y., Fan, J., Kim, Y.J.R., Lee, S.A., Ishida, E., Blaner, W.S., and Accili, D. (2016). Aldehyde dehydrogenase 1a3 defines a subset of failing pancreatic beta cells in diabetic mice. Nat. Commun. *7*, 12631. https://doi.org/10.1038/ncomms12631.
28. Bartolome, A., Zhu, C., Sussel, L., and Pajvani, U.B. (2019). Notch signaling dynamically regulates adult beta cell proliferation and maturity. J. Clin. Invest. *129*, 268–280. https://doi.org/10.1172/JCI98098.
29. Bar, Y., Russ, H.A., Sintov, E., Anker-Kitai, L., Knoller, S., and Efrat, S. (2012). Redifferentiation of expanded human pancreatic β cell-derived cells by inhibition of the NOTCH pathway. J. Biol. Chem. *287*, 17269–17280. https://doi.org/10.1074/jbc.M111.319152.
30. Bar, Y., Russ, H.A., Knoller, S., Ouziel-Yahalom, L., and Efrat, S. (2008). HES-1 is involved in adaptation of adult human beta-cells to proliferation *in vitro*. Diabetes *57*, 2413–2420. https://doi.org/10.2337/db07-1323.
31. Saunders, D.C., Aamodt, K.I., Richardson, T.M., Hopkirk, A.J., Aramandla, R., Poffenberger, G., Jenkins, R., Flaherty, D.K., Prasad, N., Levy, S.E., et al. (2021). Coordinated interactions between endothelial cells and macrophages in the islet microenvironment promote β cell regeneration. NPJ Regen. Med. *6*, 22. https://doi.org/10.1038/s41536-021-00129-z.
32. Diedisheim, M., Oshima, M., Albagli, O., Huldt, C.W., Ahlstedt, I., Clausen, M., Menon, S., Aivazidis, A., Andreasson, A.C., Haynes, W.G., et al. (2018). Modeling human pancreatic beta cell dedifferentiation. Mol. Metabol. *10*, 74–86. https://doi.org/10.1016/j.molmet.2018.02.002.
33. Maddaluno, L., Urwyler, C., and Werner, S. (2017). Fibroblast growth factors: key players in regeneration and tissue repair. Development *144*, 4047–4060. https://doi.org/10.1242/dev.152587.
34. Minami, K., Yano, H., Miki, T., Nagashima, K., Wang, C.Z., Tanaka, H., Miyazaki, J.I., and Seino, S. (2000). Insulin secretion and differential gene expression in glucose-responsive and -unresponsive MIN6 sublines. Am. J. Physiol. Endocrinol. Metab. *279*, E773–E781. https://doi.org/10.1152/ajpendo.2000.279.4.E773.
35. Kitamoto, T., Sakurai, K., Lee, E.Y., Yokote, K., Accili, D., and Miki, T. (2018). Distinct roles of systemic and local actions of insulin on pancreatic β cells. Metabolism *82*, 100–110. https://doi.org/10.1016/j.metabol.2017.12.017.

STAR★METHODS

KEY RESOURCES TABLE

REAGENT or RESOURCE	SOURCE	IDENTIFIER
Antibodies		
insulin	abcam	#ab7842; RRID: AB_306130
glucagon	CST	#2760; RRID: AB_659831
Glucagon (K79bB10)	Sigma-Aldrich	#G2654; RRID: AB_259852
RFP	MBL	#PM005; RRID: AB_591279
RFP	ChromoTek	#5F8; RRID: AB_2336064
Aldh1a3	Novus Biologicals	#NBP2-15339; RRID: AB_2665496
MafA	Bethyl laboratories	#IHC-00352; RRID: AB_1279486
MafB	Bethyl laboratories	#BLR046F; RRID: AB_2891845
BrdU	abcam	#ab6326; RRID: AB_305426
Ki67	abcam	#ab15580; RRID: AB_443209
Ki67 (TEC-3)	Dako	M7249; RRID: AB_2250503
Hes1	abcam	#ab108937; RRID: AB_10862625
Ngn3	Developmental Studies Hybridoma Bank	#F25A1B3; RRID: AB_528401
MASH1 (Ascl1)	BD Pharmingen	#556604; RRID: AB_396479
Somatostatin (Sst)	Proteintec	#24496-1-AP; RRID: AB_2918083
Alexa Fluor 488 Goat anti Rabbit	Thermo Fisher	#A-11008; RRID: AB_143165
Alexa Fluor 555 Goat anti Rabbit	Thermo Fisher	#A-21428; RRID: AB_141784
Alexa Fluor 633 Goat anti Rabbit	Thermo Fisher	#A-21070; RRID: AB_2535731
Alexa Fluor 488 Goat anti Guinea pig	Thermo Fisher	#A-11073; RRID: AB_2534117
Alexa Fluor 555 Goat anti Guinea pig	Thermo Fisher	#A-21435; RRID: AB_2535856
Alexa Fluor 633 Goat anti Guinea pig	Thermo Fisher	#A-21105; RRID: AB_2535757
Alexa Fluor 488 Goat anti Mouse	Thermo Fisher	#A-11001; RRID: AB_2534069
Alexa Fluor 633 Goat anti Mouse	Thermo Fisher	#A-21052; RRID: AB_2535719
Alexa Fluor 633 Goat anti Rat	Thermo Fisher	#A-21094; RRID: AB_141553
Polyclonal Goat anti Rabbit HRP	Dako	#P0448; RRID: AB_2617138
Polyclonal Goat anti Mouse HRP	Dako	#P0447; RRID: AB_2617137
Chemicals, peptides, and recombinant proteins		
Diphtheria toxin	Merck Millipore	#322326
5-Bromo-20-deoxyuridine (BrdU)	Wako pure chemical inc	#027-15561
5-Ethynyl-2′-deoxyuridine (EdU)	Thermo Fisher	#A10044
D-MEM, high glucose	Wako Pure Chemical	#044-29765
Penicillin-Streptomycin	Wako Pure Chemical	#161-23181
Fetal bovine serum	biowest	#S1560
Gelatin	Wako Pure Chemical	#077-03155
Hematoxylin	Wako Pure Chemical	#131-09965
Eosin Y	Wako Pure Chemical	#058-00062
Ethanol	Wako Pure Chemical	#057-00451
Isopropanol	Wako Pure Chemical	#321-00047
Chloroform	Wako Pure Chemical	#038-02606
Methanol	Wako Pure Chemical	#139-01827
Xylene	Wako Pure Chemical	#244-00081

(*Continued on next page*)

Continued

REAGENT or RESOURCE	SOURCE	IDENTIFIER
Paraffin	Sakura-finetek	#7810
OCT compound	Sakura-finetek	#4583
Formaldehyde solution	Wako Pure Chemical	#064-00401
Hoechst	Tocris Bioscience	#5117/50
Critical commercial assays		
PEN membrane Glass slides	Thermo Fischer	#LCM-0522
Arcturus Picopure RNA isolation kit	Applied Biosystems	#KIT-0204
CapSure Macro LCM Caps	Thermo Fischer	#LCM-0211
ReverTra Ace	TOYOBO	#TRT-101
Fast SYBR green	Applied Biosystems	#4385612
Click-iT™ Plus EdU Cell Proliferation Kit for Imaging, Alexa Fluor 488	Invitrogen	#C10637
TSA-fluorescein	PerkinElmer	#NEL741001KT
Experimental models: Cell lines		
MIN6 cells	Minami et al. (2000)[34]	N/A
Experimental models: Organisms/strains		
Rip-Cre: (Postic et al. 1999)[18]	Jackson Laboratory	#003573
Rosa26$^{iDTR/+}$	Jackson Laboratory	#008040
Rosa26$^{tdtomato/+}$	Jackson Laboratory	#007914
Oligonucleotides		
Hprt forward: 5′-GCGTCGTGATTAGCGATGA-3′	Lee EY et al. (2015)[1]	N/A
Hprt reverse: 5′-ATGGCCTCCCATCTCCTT-3′	Lee EY et al. (2015)[1]	N/A
Ins2 forward: 5′-ACCCACAAGTGGCACAACTG-3′	This paper	N/A
Ins2 reverse: 5′-GCACTGATCTACAATGCCAC-3′	This paper	N/A
Mki67 forward: 5′-CAGATGAGGTGATACAGGCTC-3′	This paper	N/A
Mki67 reverse: 5′-TCCGAGTACTGGATAGCAC-3′	This paper	N/A
MafA forward: 5′-GAGGAGGTCATCCGACTGAAA-3′	This paper	N/A
MafA reverse: 5′-GCACTTCTCGCTCTCCAGA-3′	This paper	N/A
MafB forward: 5′-GAACGAGAAGACGCAGCT-3′	This paper	N/A
MafB reverse: 5′-CGAGTTTCTCGCACTTGACCT-3′	This paper	N/A
Neurog3 forward: 5′-GTCGGGAGAACTAGGATGGC-3′	This paper	N/A
Neurog3 reverse: 5′-GGAGCAGTCCCTAGGTATG-3′	This paper	N/A
Aldh1a3 forward: 5′-GGGTCACACTGGAGCTAGGA-3′	This paper	N/A
Aldh1a3 reverse: 5′-CTGGCCTCTTCTTGGCGAA-3′	This paper	N/A
Hes1 forward: 5′-AAAGACGGCCTCTGAGCAC-3′	This paper	N/A
*Hes1*reverse: 5′-GGTGCTTCACAGTCATTTCCA-3′	This paper	N/A
Fgf2 forward: 5′-CCAACCGGTACCTTGCTATG-3′	This paper	N/A
Fgf2 reverse: 5′-ACTGCCAGTTCGTTTCAGT-3′	This paper	N/A
Arx forward: 5′-GCTCTCCTCCTACTGCATCG-3′	This paper	N/A
Arx reverse: 5′-GTGCAGCTCAGCCTCGAA-3′	This paper	N/A
Gcg forward: 5′-AGGGACCTTTACCAGTGATGT-3′	This paper	N/A
Gcg reverse: 5′-AATGGCGACTTCTTCTGGGAA-3′	This paper	N/A
Software and algorithms		
Graphpad Prism 8	MDF	N/A
BZ-X analyzer	Keyence	N/A
FLUOVIEW	Olympus	N/A

EXPERIMENTAL MODEL AND STUDY PARTICIPANT DETAILS

Animals

Rip-Cre:Rosa26$^{DTR/tdTomato}$ mice (DTR mice) that express DTR and a fluorescent protein (tdTomato) specifically in β-cells were generated as previously reported.[19] *Rosa26*$^{DTR/+}$ mice and Rosa26$^{tdTomato/+}$ were purchased from The Jackson Laboratory. Rat insulin promoter-Cre (Rip-Cre) transgenic mice were crossbred with Rosa26$^{DTR/+}$ mice and Rosa26$^{tdTomato/+}$ mice to generate Rip-Cre; Rosa26$^{DTR/tdTomato}$ mice. Male mice aged 8 to 12 weeks were used in the study. The mice were housed in a climate-controlled room with a temperature of 23 ± 3°C, humidity of 55 ± 15 %, and a 12 h light/12 h dark cycle and fed standard laboratory chow (CE-2; Clea Japan Inc., Tokyo, Japan) *ad libitum*. All animal experiments were approved by the Animal Care Committee of Chiba University.

METHOD DETAILS

All methods can be found in the accompanying transparent methods supplemental file.

Antibodies

The following antibodies were used for immunostaining. Guinea pig anti-insulin (1:100; ab7802, Abcam), rabbit anti-glucagon (1:200; #2760, CST), mouse anti-glucagon (1:2,000; K79bB10, Sigma Aldrich), rabbit anti-RFP (1:2,000; PM005, MBL), rat anti-RFP (1:1,00; 5F8, ChromoTek), rabbit anti-Aldh1a3 (1:400; NBP2-15339, Novus Biologicals), rabbit anti-MafA (1:100; IHC-00352, Bethyl laboratories), rabbit anti-MafB (1:100; BLR046F, Bethyl laboratories), rat anti-BrdU (1:100; ab326, Abcam), rabbit anti-Ki67 (1:50; ab15580, Abcam), rat anti-Ki67 (1:50; DAKO), rabbit anti-Hes1 (1:100; ab108937, abcam), mouse anti-MASH1(Ascl1) (1:100; #556604, BD biosciences), rabbit anti-Sst (1:500; #24496-1-AP, Proteintec).

Animal models

For genetic β-cell ablation, DTR mice received a single intraperitoneal injection of 40 μg/kg DT at daytime (10:00–17:00). Pancreata were excised 6 or 14 days later and subjected to immunohistochemical analyses and laser capture microdissection for quantitative RT-PCR (RT-qPCR) analysis. For surgical reduction of β-cells, partial pancreatectomy was performed. Under anesthesia by inhalation of 1.7 ∼ 1.9 % isoflurane (DS Pharma Animal Health Co. Ltd., Osaka, Japan), the abdomen of the mice was opened by a left lateral incision. ∼70% pancreatectomy was performed by surgical removal of the entire splenic portion and a part of the intestinal portion of the pancreas and spleen. Splenectomy was performed in control mice to avoid influence of splenocytes. Total pancreas weight of the mouse to be pancreatectomized was estimated from its body weight; the weight of the excised pancreas tissues was based on this calculation. For sampling, the pancreata were excised 6 or 14 days after surgery and subjected to immunohistochemistry or laser capture microdissection (for RT-qPCR analysis).

Labeling of proliferating cells

For EdU incorporation analysis, the mice were labeled with 250 μg/mL EdU dissolved in drinking water for 6 days or 14 days and EdU incorporated in the cellular nuclei in the pancreata was visualized by click chemistry (Thermo Fischer Scientific Inc). Blood glucose levels at the indicated time points were measured using Glutestmint (Sanwa Kagaku Kenkyusho Co. Ltd.). To quantify repetitive β-cell proliferation after DT treatment or PPx, the mice were sequentially administered EdU and BrdU. Briefly, the mice underwent 6-day-labeling with EdU after DT administration or PPx (Day 1-Day 6) followed by a 1-day-interval for EdU-washout (Day 7) and 3-day-labelling with 1 mg/mL BrdU (Day 8-10). The pancreata were then excised and subjected to immunohistochemical analyses.

Preparation of pseudo-islets and transplantation

Pseudo-islets were prepared as previously reported.[35] Briefly, 20 μL MIN6 cell suspension (1.5 × 10^4 cells/mL) in DMEM (25 mM glucose) was cultured in a hanging drop for 3 days and the cell spheres were then transferred to a gelatin (1%)-coated dish and cultured for another 3 days before transplantation. Pseudo-islets were transplanted to the sub-renal capsule of eight-week-old male mice. One week after pseudo-islet transplantation, β cell ablation by DT treatment or PPx was performed; the pancreata were excised 14 days later.

Histological analysis

Extracted pancreata were fixed and embedded in paraffin, and 4 μm sections were cut. For quantitative analysis of islet mass and the number of specific cell types, the whole paraffin-embedded pancreas was cut into sections spaced 160 μm apart. Eleven to 14 sections of each pancreas were stained with hematoxylin–eosin (HE) or immunostained. Immunofluorescence of transcriptional factors including MafA, MafB, and Hes1 was visualized by TSA fluorescence system (PerkinElmer, Waltham, MA) according to the manufacturer's instructions. To calculate the number of a specific cell type, histological images of the islets were obtained by FV10i confocal microscope (Olympus, Tokyo, Japan) and the cells positive for immunoreactivity were counted. Islet mass was calculated by multiplying total weight of the pancreas by the ratio of the islet cell area to the pancreas area. The number of islet cells in the pancreas was calculated by multiplying (1) the total Hoechst33342-positive cell number in the islets of all sections by (2) the ratio of the sum of islet cell area to the sum of pancreas area and

by (3) the pancreas weight [islet cell number = (1) × (2) × (3)]. Hoechst33342 was purchased from Sigma, St. Louis, MO, USA. The number of a specific cell type (*i.e.*, insulin-positive, Tomato-positive, EdU- or BrdU-positive cells) was calculated similarly.

The relative percentage was calculated by dividing the number of labeled cells by the number of total nuclei in the islet, and then multiplying the result by 100. Mean cell area was calculated by dividing the islet area by the number of total nuclei in the islet.

Laser capture microdissection of islets

Excised pancreata were embedded in OCT compound and frozen immediately in liquid nitrogen. Cryosections were cut 20 μm thick and mounted on PEN membrane Glass slides (Thermo Fisher) in a RNase-free container. Sections were briefly stained with hematoxylin (Vector Laboratories) for 3 sec and then dehydrated in ethanol and dried in air for laser capture microdissection.

LCM was performed using a laser microdissection system from Applied biosystems Arcturus XT LCM systems (Applied Biosystems). 50 to 100 islets were collected from each mouse; cut elements were catapulted into CapSure Macro LCM Caps (Applied Biosystems) resuspended in Extraction buffer. Total RNA was extracted immediately using an Arcturus Picopure RNA isolation kit following the manufacturer's protocol. Reverse transcription was performed using ReverTra Ace (ToYoBo). Quantitative real-time PCR was performed under the standardized protocol as previously reported.[1] The primers used were listed in key resources table.

QUANTIFICATION AND STATISTICAL ANALYSIS

Values are mean ± SEM. Statistical analyses were performed using GraphPad Prism8 (GraphPad Software Inc., La Jolla, CA, USA). Comparison between two groups was assessed using unpaired Student's t-test for normally distributed variables. Multiple comparison was done using one-way ANOVA followed by Dunnett's or Tukey's post-hoc test. To clarify the relationship between two variables, Pearson's correlation coefficient was used. P values were considered significant at $P < 0.05$.